

Document downloaded from:

<http://hdl.handle.net/10251/160902>

This paper must be cited as:

Robles Martínez, Á.; Capson-Tojo, G.; Gales, A.; Viruela, A.; Sialve, B.; Seco, A.; Steyer, J.... (2020). Performance of a membrane-coupled high-rate algal pond for urban wastewater treatment at demonstration scale. *Bioresource Technology*. 301:1-10.
<https://doi.org/10.1016/j.biortech.2019.122672>



The final publication is available at

<https://doi.org/10.1016/j.biortech.2019.122672>

Copyright Elsevier

Additional Information

1 **Performance of a membrane-coupled high-rate algal pond for urban wastewater**
2 **treatment at demonstration scale**

3 Ángel Robles ^{a,*}, Gabriel Capson-Tojo ^b, Amandine Gales ^c, Alexandre Viruela ^d, Bruno
4 Sialve ^c, Aurora Seco ^a, Jean-Philippe Steyer ^c, José Ferrer ^d

5
6 ^a Departament d'Enginyeria Química, Escola Tècnica Superior d'Enginyeria, Universitat de
7 València, Avinguda de la Universitat s/n, 46100 Burjassot, Valencia, Spain

8 ^b CRETUS Institute, Department of Chemical Engineering, School of Engineering,
9 Universidade de Santiago de Compostela, 15782, Santiago de Compostela, Spain

10 ^c LBE, Univ. Montpellier, INRA, 102 avenue des Etangs, 11100, Narbonne, France

11 ^d Institut Universitari d'Investigació d'Enginyeria de l'Aigua i Medi Ambient (IIAMA).
12 Universitat Politècnica de València. Camí de Vera s/n. 46022. Valencia. Spain.

13 * Corresponding author: tel. +34 96 354 30 85, e-mail: *angel.robles@uv.es*

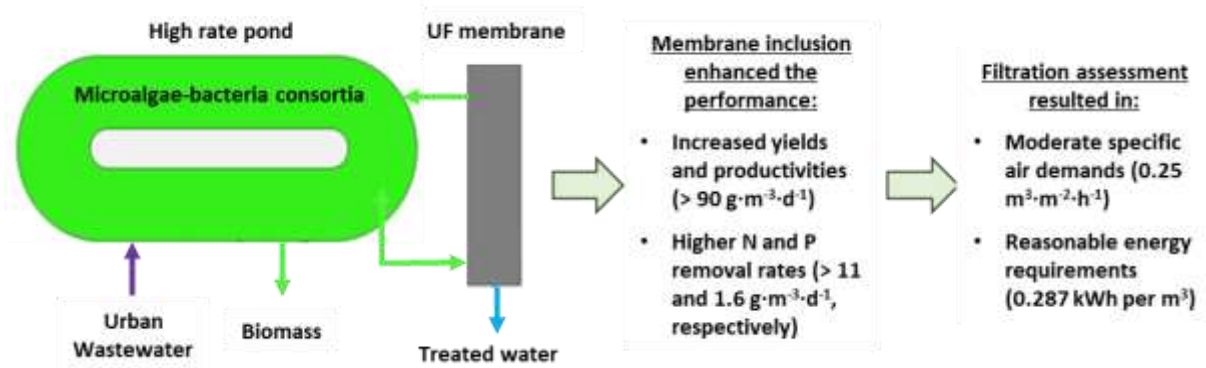
14
15 **Abstract**

16 The objective of this study was to evaluate the performance of an outdoor membrane-coupled
17 high-rate algal pond equipped with industrial-scale membranes for treating urban wastewater.
18 Decoupling biomass retention time (BRT) and hydraulic retention time (HRT) by membrane
19 filtration resulted in improved process efficiencies, with higher biomass productivities and
20 nutrient removal rates when operating at low HRTs. At 6 days of BRT, biomass productivity
21 increased from 30 to 65 and to 90 g·m⁻³·d⁻¹ when operating at HRTs of 6, 4 and 2.5 days,
22 respectively. The correspondent nitrogen removal rates were 4, 8 and 11 g N·m⁻³·d⁻¹ and the
23 phosphorous removal rates were 0.5, 1.3 and 1.6 g P·m⁻³·d⁻¹. The system was operated
24 keeping moderate specific air demands (0.25 m³·m⁻²·h⁻¹), resulting in reasonable operating

25 and maintenance costs (€0.04 per m³) and energy requirements (0.287 kWh per m³). The
26 produced water was free of pathogens and could be directly used for reusing purposes.

27

28 Graphical abstract



29

30

31 Keywords

32 HRAP; nutrient recovery; ultrafiltration; hollow-fibre membranes; industrial-scale

33

34 Highlights

- 35 • Decoupling hydraulic and biomass retention times increased the system performance
- 36 • Low HRTs enhanced N and P removal rates (up to 11 g N·m⁻³·d⁻¹ and 1.6 g P·m⁻³·d⁻¹)
- 37 • Efficient operation achieved at low specific air demands (0.25 m³·m⁻²·h⁻¹)
- 38 • Relatively low operational energy requirements (0.287 kWh per m³)

39

40 1. Introduction

41 The concept of circular economy relies on the recovery of valuable compounds from waste
42 streams. To implement this approach, wastewater treatment plants are nowadays being shifted
43 towards modern water resource recovery facilities (WRRFs), where the wastewater is not only
44 treated and disposed, but also transformed into valuable products (*e.g.* energy, nutrients and

45 reclaimed water).

46 The recovery of nutrients from urban wastewater (UWW) is a key goal to be achieved in
47 future WRRFs due to its essential role in achieving a sustainable food production-
48 consumption network. Microalgae-based processes have a huge potential as main actors for
49 this purpose (Salama et al., 2017). Autotrophic microalgae are organisms able to grow using
50 carbon dioxide as carbon source and light as energy source, assimilating at the same time the
51 nutrients required for their growth (*i.e.* inorganic nitrogen and phosphorous). They convert
52 these materials into biomass and a series of valuable organic compounds which are
53 precursors of different forms of bio-energy (*e.g.* biogas, biodiesel, bio-ethanol, and bio-
54 butanol) and other value-added products (*e.g.* products for livestock or fertilizers) (Wang et
55 al., 2016). The cultivation of microalgae in wastewaters could reduce the production costs,
56 generating at the same time clean water, recovering the nutrients initially present in the
57 wastewater and capturing carbon dioxide during their growth by harvesting solar energy, thus
58 reducing the environmental impact of the process (Wang et al., 2016). However, while these
59 autotrophic microorganisms can efficiently reduce the concentrations of nutrients present in
60 wastewater to very low values (*e.g.* 2.20 mg NH₄-N·L⁻¹ and 0.15 mg PO₄-P·L⁻¹ (Boelee et al.,
61 2011)), they cannot remove organic matter, thus not being able to provide a complete
62 wastewater treatment. Because of this, microalgae-based treatment systems are generally
63 applied for tertiary wastewater treatment or are often combined with anaerobic pretreatments
64 (Wang et al., 2015).

65 The utilization of microalgae-bacteria consortia to provide a complete single-stage treatment
66 of wastewater is regarded as a potential solution for this problem. This wastewater treatment
67 approach is based upon a synergetic interaction: the organic matter is degraded by
68 heterotrophic bacteria, producing carbon dioxide, which is consumed by microalgae during
69 photosynthesis, assimilating nutrients during this process and generating the oxygen that

70 bacteria need to carry out aerobic respiration. In addition, other advantages of this mixed-
71 culture systems have been postulated when compared to sole-microalgae cultures: (i) algae
72 and bacteria produce vitamins and other organic compounds which can be beneficial for the
73 growth of the partners, (ii) some microalgae generate a extracellular matrix that can provide
74 attachment sites for bacteria and be used as carbon source, (iii) bacteria have been found to
75 favour the flocculation of algae, enhancing biomass harvesting and (iv) the spatial distance for
76 oxygen and carbon dioxide exchange is decreased (Arbib et al., 2017; Fernández-Sevilla et
77 al., 2018; Galès et al., 2019; Liao et al., 2018; Shoener et al., 2019; Wang et al., 2016). Recent
78 studies have demonstrated the feasibility of microalgae-bacteria consortia for UWW
79 treatment. Removals of 92% of the biological chemical demand (BOD), 75% of the total
80 nitrogen (N_T) and 93% of total phosphorus (P_T) have been reported using offshore
81 photobioreactors (PBRs) (Novoveská et al., 2016). Photo-sequencing batch reactors reached
82 removals of 87% of the chemical oxygen demand (COD) and 98% of the total Kjeldahl
83 nitrogen (TKN), without the need of external aeration (Foladori et al., 2018). In high-rate
84 algal ponds (HRAPs), removal efficiencies of 40-80% of the soluble COD, 80-100% of the
85 NH_4^+ and 30-80% of the PO_4^{3-} have been reported (Galès et al., 2019). Therefore, these
86 systems have appeared as an environmental-friendly wastewater treatment option able to
87 remove both COD and nutrients while avoiding the need of supplying external oxygen or
88 carbon dioxide.

89 Two key factors are limiting the application of microalgae-bacteria consortia for UWW
90 treatment: (i) high amounts of total suspended solids (TSS) in the effluent (washout of
91 microorganisms) and (ii) expensive biomass harvesting methods (Craggs et al., 2011;
92 Solimeno and García, 2017; Wang et al., 2016). Both of these issues could be overcome by
93 using membranes for biomass retention, enabling the decoupling of the biomass retention time
94 (BRT) and the hydraulic retention time (HRT) (Bhave et al., 2012; González-Camejo et al.,

95 2019; Liao et al., 2018; Seco et al., 2018; Viruela et al., 2018). The application of membranes
96 also provides an efficient solid-liquid separation, acting as biomass harvesting process and
97 resulting in increased biomass concentrations and higher productivities due to enhanced
98 nutrient removal efficiencies and higher organic loading rates (Bilad et al., 2014b; Honda et
99 al., 2012; Luo et al., 2017). Furthermore, the addition of ultrafiltration membranes allows
100 producing reclaimed water (*i.e.* with negligible levels of pathogens and suspended solids)
101 from wastewater, directly applicable for several purposes (*e.g.* irrigation or fertirrigation,
102 aquifer recharge or urban/industrial uses).

103 HRAPs have been widely applied for large-scale cultivation of microalgae worldwide, mainly
104 due to their low investment and operational costs, their easy operation and maintenance and
105 their low specific energy demand (Craggs et al., 2011; Kumar et al., 2015). Coupling
106 membranes and HRAP can also help to overcome the low biomass productivities achieved,
107 which has been recognised as a key challenge in HRAPs (Craggs et al., 2011; Dalrymple et
108 al., 2013; Drexler and Yeh, 2014). Nevertheless, before membrane-coupled high-rate algal
109 ponds (M-HRAP) can be applied industrially, research must still be carried out to ensure the
110 feasibility of this technology (Bilad et al., 2014a). A key challenge that this technology may
111 face is membrane fouling (Bilad et al., 2012; Marbelia et al., 2014; Sun et al., 2013;
112 Wicaksana et al., 2012). In addition, the performance of M-HRAPs for wastewater treatment
113 is significantly sensitive to the environmental and operating conditions, which must be
114 optimized for each particular case. The available literature dealing with urban wastewater
115 treatment via microalgae-bacteria consortia using membranes for decoupling BRT and HRT is
116 limited, with no pilot/demonstration-scale studies available using HRAPs. Therefore, the
117 performance and feasibility of this process must be evaluated, determining the achievable
118 biomass productivities and the resulting nutrient recoveries. Potential operational issues must
119 still be identified, setting the baselines for future optimization.

120 The objective of this study was to evaluate the performance of an outdoor M-HRAP equipped
121 with industrial-scale membranes for treating UWW. The effect of the membrane addition to
122 the HRAP system (decoupling of BRT and HRT) on the treatment performance was assessed.
123 In addition, the effect of naturally varying environmental conditions (*i.e.* temperature and
124 light intensity) on the outdoor M-HRAP performance were also studied. The capability of the
125 process for UWW treatment was evaluated by determining the biomass productivities, the
126 nutrient removal rates and the COD removal efficiencies, all of them being crucial parameters
127 for these systems. After assessing the filtration performance, energetic and economic analyses
128 were carried out to study the potential feasibility on the proposed process.

129

130 **2. Materials and methods**

131 *2.1. Self-inoculation of the HRAP and influent wastewater*

132 The plant was self-inoculated after starting feeding it with UWW. The start-up period for
133 inoculation lasted for 1-2 weeks. An initial natural selection of the predominant
134 microorganisms occurred naturally, facilitating the potential application of this technology.
135 *Scenedesmus obliquus* was the predominant microalgal strain within the different runs, with a
136 relative abundance of around 70, 90 and up to 100% in runs 1, 2 and 3-4 (see Table 1),
137 respectively. Synthetic UWW was used as substrate for microbial growth. This UWW was
138 prepared according to Nopens et al. (2001) and contained 332 ± 55 mg COD·L⁻¹, 89 ± 24 mg·L⁻¹
139 of volatile suspended solids (VSS), 17.3 ± 8.1 mg N·L⁻¹ of NH₄-N (45.5 ± 24.2 mg N·L⁻¹ N_T)
140 and 3.9 ± 1.6 mg P·L⁻¹ of PO₄-P (6.1 ± 2.2 mg P·L⁻¹ P_T). It was continuously fed to the HRAP
141 from a refrigerated tank (kept at 4 °C) with a volume of 500 L.

142 *2.2. Description of the demonstration plant (M-HRAP)*

143 A continuously-operated M-HRAP was used in this study. Its working volume was 22 m³,
144 with a depth of 0.3 m and a solar irradiance area of approximately 73.4 m². The HRAP

145 (located in the south of France, Lat. 43.156711, Long. 2.995075) was continuously mixed by
146 a paddlewheel. The HRAP was connected to two membrane tanks (MT1 and MT2), each of
147 them including one membrane bundle (with a filtration area of 3.44 m²) that was obtained
148 from one industrial-scale hollow-fibre ultrafiltration membrane unit (PURON® Koch
149 Membrane Systems (PUR-PSH31), 0.03 µm). A flow diagram of the system can be found in
150 the supplementary material.

151 *2.3. Monitoring of the plant operation*

152 Different on-line sensors were installed in the M-HRAP to obtain real-time information of the
153 state of the process. The on-line sensors placed in the HRAP were: (i) a pH-T transmitter
154 (METTLER TOLEDO InPro® 4260 SG), (ii) a dissolved oxygen probe (METTLER
155 TOLEDO InPro® 6800 G Amperometric Oxygen Sensor), (iii) an ultrasonic flowmeter for
156 determining the influent flowrate (Titan Enterprises Ltd. atrato), and (iv) an irradiation sensor
157 (Skye PAR Quantum Sensor) for measuring the photosynthetic active radiation (PAR).
158 Moreover, several sensors were installed to monitor the membrane performance: two liquid
159 flow-rate transmitters (one after the mixed liquor recycling pump and another after the
160 permeate pump), three level transmitters (one for each membrane tank and another for the
161 clean-in-place unit), one pressure transmitter for monitoring the transmembrane pressure in
162 the membrane tanks, one air pressure transmitter (in the blower outlet) and one air flowmeter
163 for measuring the air sparging for membrane scouring. The T and PAR values provided in this
164 work refer to daily averages of the continuous PAR measurements, considering both daylight
165 and night-time hours.

166 In addition to the on-line process monitoring, samples were taken three times per week from
167 the influent, the mixed liquor and the effluent streams to evaluate the performance of the
168 biological processes. The concentrations of the total and soluble COD (COD_{TOT} and COD_S,
169 respectively), N_T, P_T, inorganic nutrients (NH₄⁺, NO₂⁻, NO₃⁻ and PO₄⁻³), total suspended solids

170 (TSS) and VSS were periodically measured. In addition, the optical density at 680 nm (OD_{680})
171 was used for VSS estimation. The structure of the microbial community was studied via the
172 estimation of the eukaryotic and prokaryotic cell numbers by quantitative polymerase chain
173 reaction (qPCR). The presence of microalgal biomass was estimated targeting a partial
174 sequence of 18S rDNA from chlorophyte or bacillariophyte, whilst the total bacterial content
175 was estimated using universal primers and probes for the 16S rDNA. A more extended
176 description can be found in Turon et al. (2015).

177

178 2.4. Operation of the plant

179 The M-HRAP was operated outdoors (*i.e.* under ambient temperature and solar irradiance
180 conditions) at a constant BRT of 6 days and three different HRTs: 6 days (run I; no membrane
181 operation), 4 days (run II) and 2.5 days (run III). As the temperature and the light irradiation
182 are known to affect significantly the performance of microalgae-based wastewater treatment
183 processes (Perin et al., 2016; Ras et al., 2013), the influence of these variables on the M-
184 HRAP was studied during run IV (at equivalent BRT and HRT as run III). Table 1 shows the
185 particular objective of each run period, as well as the applied working conditions and the daily
186 average solar irradiances and culture temperatures.

187

188 The membrane was operated with a gross transmembrane flux (J) of $28 \text{ L}\cdot\text{m}^{-2}\cdot\text{h}^{-1}$ (LMH) at
189 the beginning of run II, lowering its value to 14 LMH afterwards. The value of J was fixed at
190 28 LMH during run III, varying between 27-31 LMH in run IV. During run II, the average
191 specific air demand per square meter of membrane area (SAD_m) was set to $0.3 \text{ m}^3\cdot\text{m}^{-2}\cdot\text{h}^{-1}$ and
192 then increased to $0.6 \text{ m}^3\cdot\text{m}^{-2}\cdot\text{h}^{-1}$ to maintain the desired J . The SAD_m varied from 0.12-1.0
193 $\text{m}^3\cdot\text{m}^{-2}\cdot\text{h}^{-1}$ and 0.6-1.2 $\text{m}^3\cdot\text{m}^{-2}\cdot\text{h}^{-1}$ during run III and IV, respectively. The pH varied freely
194 according to variations in the carbon dioxide concentrations, related to the activity of

195 microorganisms.

196 2.5. Analytical methods and microbial analysis

197 The concentrations of COD_{TOT}, COD_S, N_T, P_T and VSS were measured according to the
198 Standard Methods (APHA, 2005). The concentrations of nutrients, *i.e.* NH₄⁺, NO₂⁻, NO₃⁻ and
199 PO₄³⁻, were determined by ion chromatography, according to Capson-Tojo et al. (2017).

200 2.6. Data treatment and calculations

201 To evaluate the performance of the M-HRAP treatment process, the nitrogen removal rate
202 (NRR), the phosphorus removal rate (PRR) and the biomass productivity were calculated
203 according to Equations 1 to 3:

204

$$205 \quad NRR = \frac{Q \cdot (N_i - N_e)}{V_{MHRAP}} \quad \text{Eq. 1}$$

$$206 \quad PRR = \frac{Q \cdot (P_i - P_e)}{V_{MHRAP}} \quad \text{Eq. 2}$$

$$207 \quad \text{Biomass productivity} = \frac{Q_w \cdot X_{VSS}}{V_{MHRAP}} \quad \text{Eq. 3}$$

208

209 Where, Q is the treatment flow rate (m³·d⁻¹), N_i is the concentration of nitrogen in the influent
210 (g N·m⁻³), N_e is the concentration of nitrogen in the effluent (g N·m⁻³), V_{MHRAP} (m³) is the
211 total volume of the M-HRAP, P_i is the concentration of phosphorus in the influent (g P·m⁻³),
212 P_e is the concentration of phosphorus in the effluent (g P·m⁻³), Q_w (m³·d⁻¹) is the flow rate of
213 wasted biomass and X_{VSS} (g VSS·m⁻³) is the VSS concentration in the HRAP.

214 The photosynthetic efficiency (PE), and the carbon dioxide biofixation (CO_{2BF}) (kg CO₂ per
215 m³ of treated water) were also used as indicator of the biological activity. They were
216 calculated according to Eq. 4, and Eq. 5, respectively.

217

218
$$PE (\%) = \frac{r_G \cdot H_B}{I \cdot S \cdot f} \cdot 100$$
 Eq. 4

219
$$CO_{2BF} = \frac{r_G}{Y_{CO_2} \cdot Q}$$
 Eq. 5

220

221 Where r_G is the daily microalgae growth (kg VSS·d⁻¹), H_B is the lower heating value of dry
222 biomass (22,900 kJ·kg VSS⁻¹), I is the PAR ($\mu\text{mol photons}\cdot\text{m}^{-2}\cdot\text{s}^{-1}$), f is a conversion factor
223 (18.78 kJ·s· $\mu\text{mol photons}^{-1}\cdot\text{d}^{-1}$), S is the surface of the open pond (m²) and Y_{CO_2} is the
224 stoichiometric CO₂ capture for microalgae growth (0.52 kg VSS·kg CO₂⁻¹). For stoichiometric
225 calculations of microalgae biomass composition, the chemical formula used in Viruela et al.
226 (2018) was applied in this study (*i.e.* C₁₀₆H₁₈₁O₄₅N₁₆P).

227

228 The measured J values were standardized to 20 °C, according to Eq. 6:

229

230
$$J_{20} = J \cdot e^{-0.0239 \cdot (T-20)}$$
 Eq. 6

231

232 Where, J_{20} is the 20 °C-standardized gross flux, J is the gross flux and T is the temperature in
233 degrees Celsius.

234 2.7. Energy and economic analysis

235 2.7.1. Power requirements

236 The energy consumption of the M-HRAP unit was assumed to be mainly related to blowers
237 (air sparging), pumps (culture media and permeate), and paddlewheel. The power
238 requirements for pumps and blower were calculated as (Pretel et al., 2016). On the other hand,
239 an energy demand of 0.4 W/m² was set for the paddlewheel.

240 2.7.2. Estimation of the operational and maintenance costs

241 The energy requirements of the blower, sludge recycling pump and permeate pump for
242 filtration or back-flushing were calculated as explained in Robles et al. (2014). The costs
243 related to energy consumption assumed an energy cost of 0.07 € per kWh, similarly to
244 average electricity prices for industrial installations in Spain.
245 Other than the energy consumption due to air sparging and permeate and culture pumping, the
246 costs related to membrane replacement and membrane chemical cleaning were considered.
247 The useful membrane lifetime was estimated from the total chlorine contact specified by the
248 manufacturer and the recommended membrane chemical cleaning frequency.
249 A more precise description of the costing methodology can be found in Robles et al. (2018).
250

251 **3. Results and discussion**

252 *3.1. Influence of the BRT and HRT decoupling on the M-HRAP performance*

253 As aforementioned, runs I-III were dedicated to study the influence of decoupling the HRT
254 and the BRT, testing different HRTs for a given BRT. Starting with runs I to III, the
255 corresponding concentrations of COD_{TOT}, COD_S, VSS and the OD measurements (together
256 with the estimated VSS) are presented in Figure 1.

257 The first observation to point out is the negligible values of the COD_S that existed in all the
258 conditions after the incubation period (always below 50 mg COD·L⁻¹). This indicates that
259 heterotrophic bacteria grew very rapidly initially, without any limitation for their growth
260 under the applied working conditions. Nevertheless, the increasing VSS and COD_{TOT}
261 concentrations that can be observed in all the figures suggest that the biomass concentration
262 augmented in the M-HRAP (considering stable COD_S contents in the influent). This suggests
263 the further development of an adapted microbial population, mainly due to growth of
264 microalgae at this point. Although the raising COD_{TOT} concentrations occurred in the three
265 run periods studied, the behaviours were clearly different. When comparing the biomass

266 concentrations in the reactors at pseudo-steady state, higher values can be observed at lower
267 HRTs (*i.e.* around 400, 500 and 600 mg VSS·L⁻¹ at HRTs of 6, 4 and 2.5 days, respectively).
268 This resulted in an enhanced general performance of the biochemical system, decreasing also
269 the time to reach a stable community. The favoured biomass growth when decoupling the
270 BRT and HRT can be attributed to two main factors: (i) the membrane avoided the wash-out
271 of microorganisms, which otherwise would have left the reactor (improving the start-up
272 process) and (ii) the increased mass flow rate of both COD and nutrients at lower HRTs
273 allowed a faster development of the microorganisms. This improvement can be easily
274 appreciated in the results presented in Table 2, where the NRRs, PRRs and biomass
275 productivities are given for each run period.

276 As this table illustrates, decoupling the BRT and the HRT increased significantly the nutrient
277 removal rates and the biomass productivities. Decreasing the HRT by a factor of 2.4 (*i.e.* from
278 6 to 2.5 days) resulted in 3-folded NRRs and PRRs when comparing runs I and III. In
279 addition, the biomass productivity increased from 30 to 65 and to 90 g VSS·m⁻³·d⁻¹ at
280 decreasing HRTs of 6, 4 and 2.5 days, respectively. The increased biological activity due to
281 BRT/HRT decoupling can also be appreciated when looking at the average pseudo-steady
282 state values of PE and CO_{2BF} during the different run periods, of 1% and 0.2 kg CO₂·m⁻³ in
283 run I, 4% and 0.3 kg CO₂·m⁻³ in run II and 3.5 % and 0.4 kg CO₂·m⁻³ in run III. Both the PE
284 and CO_{2BF} increased during the run periods following an asymptotic pattern until reaching a
285 maximum value, corresponding to the presence of a well-established microalgal community in
286 the HRAP. Interestingly, when comparing these maximum values, the PE was 4-folded and
287 the CO_{2BF} increased by 50 % between runs I and II, confirming the positive effect of biomass
288 retention. The maximum CO_{2BF} was even further increased in run III. However, the PE was
289 lower during run III when compared to run II. This is very likely caused by a shading effect
290 related to the higher biomass concentrations, decreasing the light uptake efficiency. Similar

291 phenomena have been reported previously at high HRTs (Viruela et al., 2018). This suggests
292 that an optimum combination of BRT and HRT exists, allowing to optimize the performance
293 of the system establishing efficient light uptake rates.

294 The results presented above are in agreement with previous studies focused on membrane
295 filtration coupled to outdoors microalgae-based treatment systems. Using a PBR for tertiary
296 sewage treatment at a BRT of 4.5 days and an HRT of 3.5 days, optimum conditions have
297 been reported, with a $\text{CO}_{2\text{BF}}$ of $0.55 \text{ kg CO}_2 \cdot \text{m}^{-3}$ and a PE of 2.7% (González-Camejo et al.,
298 2019). Viruela et al. (2018) also reported maximum biomass productivities, NRR and PRR
299 ($66 \text{ mg VSS} \cdot \text{L}^{-1} \cdot \text{d}^{-1}$, $7.7 \text{ mg N} \cdot \text{L}^{-1} \cdot \text{d}^{-1}$ and $1.2 \text{ mg P} \cdot \text{L}^{-1} \cdot \text{d}^{-1}$, respectively) at a BRT of 4.5
300 days. Sheng et al. (2017) also reported optimum performances at low HRTs (4 days) using
301 native microalgae in a sequencing batch membrane PBR, reaching removals of 95% and 70%
302 TN and TP, respectively. Treating synthetic wastewater with a membrane-coupled PBR
303 containing a microalgae-bacteria consortium at an HRT of 1 day, Yang et al. (2018) achieved
304 almost complete ammonium removal, with a COD removal of 90%. Using also synthetic
305 wastewater in a membrane-coupled PBR with a microalgae-bacteria consortium, Sun et al.
306 (2018) achieved 94% COD, 96% ammonia and 24% phosphate removals. The presented
307 results suggest that M-HRAPs can achieve similar (or even higher) productivities and nutrient
308 removal rates than membrane-coupled PBRs, but with lower power requirements. In this
309 respect, M-HRAP could represent an energy-efficient alternative for resource recovery
310 (energy, water and nutrients) from UWW. Nonetheless, other factors need also to be
311 addressed, such as the cost output of the recovered resources or land requirements.

312 Despite the positive effect of HRT reduction, the high nutrient loading rates into the system
313 resulted in higher concentrations of nutrients in the effluent. This fact can be appreciated in
314 Figure 2, where the evolutions of the concentrations of N_T , $\text{NH}_4\text{-N}$, $\text{PO}_4\text{-P}$, $\text{NO}_3\text{-N}$ and $\text{NO}_2\text{-N}$
315 during runs I to III are given. Nevertheless, it must be pointed out that this result was obtained

316 at a fixed BRT of 6 days. By optimizing this parameter, discharge limits could be obtained by
317 favouring a faster algae growth (González-Camejo et al., 2019).

318 As it can be observed, while the concentrations of $\text{NH}_4\text{-N}$ and $\text{PO}_4\text{-P}$ were far below 15 mg
319 $\text{N}\cdot\text{L}^{-1}$ and 2 mg $\text{P}\cdot\text{L}^{-1}$ at the end of run I, the concentrations of these species were 18 mg $\text{N}\cdot\text{L}^{-1}$
320 and 1.2 mg $\text{P}\cdot\text{L}^{-1}$ at the end of run II and 28 mg $\text{N}\cdot\text{L}^{-1}$ and over 2 mg $\text{P}\cdot\text{L}^{-1}$ at the end of run III
321 (N_T concentrations over 40 mg $\cdot\text{L}^{-1}$). This was simply related to the higher nutrient loading
322 rates caused by the lower HRTs. Besides these higher nutrient concentrations in the effluent in
323 run II, the achieved values were nearby the limits imposed by European effluent nutrient
324 standards (European directive 91/271/CEE). Considering this and the negligible amounts of
325 solids and microorganisms in the effluent from the M-HRAP, it is important to highlight that
326 this high-quality effluent is suitable for its application in multiple reuse purposes, such as
327 irrigation, fertigation, urban utilization, etc.

328 This study shows for the first time that, under the conditions applied, an M-HRAP containing
329 a microalgae-bacteria consortium can treat UWW successfully. Nevertheless, it is clear that
330 there is a great room for improvement. Control strategies aiming at optimizing the BRT and
331 HRT for the given operating conditions (*i.e.* environmental conditions and influent
332 characteristics) have a huge potential for improving the process performance (*e.g.* by
333 minimizing the values of the BRT required to maximize the biomass productivities and
334 nutrient removal rates while fulfilling the nutrients limits in the effluent).

335 Run IV served for evaluating the influence of the temperature and the light irradiation on the
336 M-HRAP performance. The weather conditions (mainly T and solar irradiance) are known to
337 have a significant effect on the performance of outdoors algae-based treatment systems, with
338 open ponds being particularly affected by seasonal variations (Mata et al., 2010). The M-
339 HRAP used in this study was run outdoors for several months, which allowed to obtain results
340 at different ambient temperatures and natural irradiances. The results presented in Table 2

341 corresponding to the plant performance during runs III and IV, show working periods with
342 equivalent working conditions but under different meteorological conditions.

343 As expected, the lower solar irradiances and temperatures during run IV (average values of
344 $253 \mu\text{E}\cdot\text{m}^{-2}\cdot\text{s}^{-1}$ and $14.1 \text{ }^\circ\text{C}$, respectively) when compared with run III ($420 \mu\text{E}\cdot\text{m}^{-2}\cdot\text{s}^{-1}$ and
345 $24.5 \text{ }^\circ\text{C}$) resulted in lower nutrients removal rates and biomass productivities. The reduction
346 on light might have lowered ATP production via photophosphorylation by algae.

347 Furthermore, lower temperatures are also known to affect the algae growth rates (Ras et al.,
348 2013). The combined effects of these parameters led to the reduction in the obtained yields.

349 Although the effect of weather patterns on the performance of the M-HRAP cannot be
350 neglected, it is interesting to consider that all the parameters used to evaluate the plant
351 performance were higher during run IV when compared to run I (see Table 2). Therefore, the
352 enhanced behaviour related to BRT/HRT decoupling (avoiding biomass wash-out) was able to
353 overcome the negative effect of lower temperatures and light availabilities.

354 *3.2. Membrane filtration performance: energy and economic analysis*

355 To assess the energy performance of the system (and thus its economic feasibility), it is
356 essential to study the membrane filtration performance. The values of J , J_{20} , SAD_m , the
357 specific air demand per permeate volume (SAD_p), the TMP and the VSS concentrations
358 during runs II and III are presented in Figure 3.

359 Low SAD_m values were maintained at the beginning of run II ($0.3 \text{ Nm}^3\cdot\text{h}^{-1}\cdot\text{m}^{-2}$), aiming at
360 keeping low energy requirements. However, the increasing VSS concentrations and
361 membrane fouling led to a TMP peak around day 10. To keep the TMP below 0.4-0.5 bar and
362 avoid membrane damage, J was lowered and the SAD_m was increased to $0.6 \text{ Nm}^3\cdot\text{h}^{-1}\cdot\text{m}^{-2}$,
363 which led to stable TMP values, but increasing the SAD_p due to the reduced J up to
364 unsustainable values (see Figure 3A and Figure 3C). The relatively small reduction in the
365 TMP after increasing the SAD_m suggests that the membrane fouling responsible for the TMP

366 peak was not caused by the formation of an easily-removable cake layer. Observations of the
367 membrane showed that, although reversible, the fouling layer consisted of a remnant viscous
368 layer, covering the surface of the membrane. This also suggests that further increasing the
369 SAD_m would not improve the membrane performance and that back-flushing was more
370 effective to clean the membrane than relaxation with air. Despite this issue, the last days of
371 operation during this run period show that the membrane can be efficiently operated at
372 relatively low SAD_m values, keeping the TMP within acceptable limits.

373 The same issue was observed during run III (Figure 3B and Figure 3D). The higher VSS
374 concentrations led to a TMP peak earlier (days 6-9), which was corrected by further
375 increasing the SAD_m , keeping the same J . Nevertheless, after a momentary drop, the TMP
376 continued to increase, even when the SAD_m was raised up to unsuitable values of around 1.2
377 $Nm^3 \cdot h^{-1} \cdot m^{-2}$, confirming that increasing the SAD_m above $0.5 Nm^3 \cdot h^{-1} \cdot m^{-2}$ did not improve the
378 filtration performance. Because of this continuous TMP raise, the membrane was manually
379 washed with water (no chemical regeneration occurred) on day 13. The instantaneous TMP
380 drop confirmed the reversible nature of the fouling layer. After membrane cleaning, it was
381 possible to keep the TMP below 0.1 bar with a SAD_m of $0.25 Nm^3 \cdot h^{-1} \cdot m^{-2}$. This operation was
382 maintained for over a week, without significant TMP increases. This suggests that it is
383 possible to operate the system with low SAD_m without applying any chemical recovery to the
384 membranes, simply by sporadically cleaning them with water.

385 As representative example, the values of J_{20} ($28 L \cdot m^{-3} \cdot h^{-1}$) and SAD_m ($0.25 m^3 \cdot m^{-2} \cdot h^{-1}$)
386 achieved during the last section of run III were used to calculate the power requirements and
387 the operational and maintenance costs of the M-HRAP. The results are presented in Figure 4.
388 The low SAD_m resulted in energy requirements for the M-HRAP of around 0.29 kWh per m^3
389 of treated water. These values are lower than those achievable for other wastewater treatment
390 methods, such as conventional activated sludge systems (0.25-0.6 kWh per m^3) or aerobic

391 membrane bioreactors (0.50-2.5 kWh per m³), pointing out the energetic feasibility of
392 proposed M-HRAP system (Lazarova et al., 2012). In addition, atmospheric nitrogen
393 activation by the Haber-Bosch process and phosphorus mining are energy intensive activities.
394 Therefore, the associated energy savings due to nutrient recovery should be considered when
395 evaluating the overall energy balance of M-HRAPs. In this respect, when energy input for
396 inorganic fertilizer production is considered, M-HRAPs can represent an energy-neutral
397 solution, significantly reducing indirect greenhouse gas emissions. Another potential factor to
398 consider in the energy balance of this technology is the produced biomass as energy carrier.
399 The microalgae harvested from the system can be used as carbon source in a side-stream
400 anaerobic digester, producing at the same time biosolids that can be used for agricultural
401 practices, representing a promising approach towards circular economy scenarios (Seco et al.,
402 2018).

403 Nonetheless, it is worth to point out that the estimations of the power requirements and the
404 costs were formulated for a full-scale plant design with a treatment capacity of 1,000 m³·d⁻¹.
405 In this regard, implementation of M-HRAP would be limited to small and decentralized
406 WRRFs due to the footprint of this technology. Indeed, significant required land is needed
407 compared to other technologies. For instance, the footprint of the biological reactor in a
408 conventional activated sludge system with a depth of water of 5 meters treating 1,000 m³·d⁻¹
409 at an HRT of 12 hours would be 100 m². The footprint of the biological reactor in an M-
410 HRAP with a depth of water of 0.3 meters treating 1,000 m³·d⁻¹ at an HRT of 2.5 days would
411 be 8,333 m². Therefore, the use of algal-based systems for UWW treatment is limited to
412 locations without land restrictions.

413 Despite the low SAD_m applied, air sparging still accounted for almost 62% of the total energy
414 requirements of the system, indicating that there is a clear room of improvement to further
415 reduce this cost. Control strategies aimed at optimising the working conditions for given

416 situations (*i.e.* HRTs, T and light intensity) have a great potential for further improving the
417 energetic costs of these systems.

418 The operational and maintenance costs (O&MCs) further reinforce the importance of reducing
419 the air sparging frequency, representing 34% of the total O&MCs. The results of the
420 economic analysis also point out that, together with air sparging, the membrane replacement
421 and its chemical cleaning account for most of the O&MC, representing 34% and 6% of the
422 total, respectively. The frequency of membrane replacement and chemical cleaning depend
423 greatly on how the plant is operated (*e.g.* the working TMP, the applied J, the VSS
424 concentrations and the BRT). Therefore, control strategies optimising the working conditions
425 can also help to reduce these costs. In addition, water could be effectively used for cleaning
426 the membranes, applying an expert control system to optimise the back-flushing effect.

427 Finally, it is worth to point out that the water produced in the the M-HRAP was free of
428 pathogens and could be directly used for reusing purposes (*i.e.* irrigation or fertirrigation).
429 Therefore, the disinfecting cost needed for ad equating the effluent from other systems (*e.g.*
430 conventional activated sludge systems) is avoided. Additionally, the benefits of resource
431 recovery (*i.e.* water, energy and nutrients) should be also considered, not only from an
432 economic point of view, but also considering social and environmental aspects. Indeed,
433 including environmental targets in production chains would result in indirect benefits,
434 enhancing the overall performance of the system, *e.g.* reducing the environmental impact of
435 phosphate mining or reducing the energy demand for chemical fertilizer production.

436

437 **4. Conclusions**

438 Decoupling BRT and HRT enhanced biomass productivities (BPs), NRR and PRR. BP
439 increased from 30 to 95 g·m⁻³·d⁻¹ when lowering the HRTs from 6 to 2.5 days (at 6 days of
440 BRT). NRR and PPR also increased from 4 to 11 g N·m⁻³·d⁻¹ and 0.5 to 1.6 g P·m⁻³·d⁻¹,

441 respectively. The system kept high BPs, NRR and PRR at lower temperatures and solar
442 irradiances. The membrane was efficiently operated at low SAD_m (around $0.25 \text{ m}^3 \cdot \text{m}^{-2} \cdot \text{h}^{-1}$),
443 resulting in adequate energy requirements ($0.287 \text{ kWh} \cdot \text{m}^{-3}$) and treatment costs ($0.04 \text{ €} \cdot \text{m}^{-3}$).
444 The produced water could be directly used for reusing purposes (*i.e.* irrigation).

445

446 **Acknowledgements**

447 The authors thank the financial support of the French National Research Agency (ANR) for
448 the “Phycover” project (project ANR-14-CE04-0011), the Spanish Ministry of Economy and
449 Competitiveness jointly with the European Regional Development Fund (project CTM2011-
450 28595-C02-01/02), and the European Climate KIC association for the “MAB 2.0” project
451 (APIN0057_2015-3.6-230_P066-05). Ángel Robles is also grateful to the Generalitat
452 Valenciana for the financial aid received via a VALi+d post-doctoral grant
453 (APOSTD/2014/049). Gabriel Capson-Tojo would like to acknowledge the Xunta de Galicia
454 for his postdoctoral fellowship (ED481B-2018/017).

455

456 **References**

- 457 APHA, 2005. Standard Methods for the Examination of Water and Wastewater. American
458 Public Health Association, Washington, DC.
- 459 Arbib, Z., de Godos, I., Ruiz, J., Perales, J.A., 2017. Optimization of pilot high rate algal
460 ponds for simultaneous nutrient removal and lipids production. *Sci. Total Environ.* 589,
461 66–72. <https://doi.org/10.1016/j.scitotenv.2017.02.206>
- 462 Bhave, R., Kuritz, T., Powell, L., Adcock, D., 2012. Membrane-based energy efficient
463 dewatering of microalgae in biofuels production and recovery of value added co-
464 products. *Environ. Sci. Technol.* 46, 5599–5606. <https://doi.org/10.1021/es204107d>
- 465 Bilad, M.R., Arafat, H.A., Vankelecom, I.F.J., 2014a. Membrane technology in microalgae
466 cultivation and harvesting: A review. *Biotechnol. Adv.* 32, 1283–1300.
467 <https://doi.org/10.1016/j.biotechadv.2014.07.008>
- 468 Bilad, M.R., Discart, V., Vandamme, D., Foubert, I., Muylaert, K., Vankelecom, I.F.J.,
469 2014b. Coupled cultivation and pre-harvesting of microalgae in a membrane
470 photobioreactor (MPBR). *Bioresour. Technol.* 155, 410–417.
471 <https://doi.org/10.1016/j.biortech.2013.05.026>

472 Bilad, M.R., Vandamme, D., Foubert, I., Muylaert, K., Vankelecom, I.F.J., 2012. Harvesting
473 microalgal biomass using submerged microfiltration membranes. *Bioresour. Technol.*
474 111, 343–352. <https://doi.org/10.1016/j.biortech.2012.02.009>

475 Boelee, N.C., Temmink, H., Janssen, M., Buisman, C.J.N., Wijffels, R.H., 2011. Nitrogen and
476 phosphorus removal from municipal wastewater effluent using microalgal biofilms.
477 *Water Res.* 45, 5925–5933. <https://doi.org/10.1016/j.watres.2011.08.044>

478 Capson-Tojo, G., Rouez, M., Crest, M., Trably, E., Steyer, J., Bernet, N., Delgenes, J.,
479 Escudié, R., 2017. Kinetic study of dry anaerobic co-digestion of food waste and
480 cardboard for methane production. *Waste Manag.* 69, 470–479.
481 <https://doi.org/10.1016/j.wasman.2017.09.002>

482 Craggs, R.J., Heubeck, S., Lundquist, T.J., Benemann, J.R., 2011. Algal biofuels from
483 wastewater treatment high rate algal ponds. *Water Sci. Technol.* 63, 660 LP – 665.

484 Dalrymple, O.K., Halfhide, T., Udom, I., Gilles, B., Wolan, J., Zhang, Q., Ergas, S., 2013.
485 Wastewater use in algae production for generation of renewable resources : a review and
486 preliminary results. *Aquat. Biosyst.* 9, 1–11.

487 Drexler, I.L.C., Yeh, D.H., 2014. Membrane applications for microalgae cultivation and
488 harvesting: a review. *Rev. Environ. Sci. Biotechnol.* 13, 487–504.
489 <https://doi.org/10.1007/s11157-014-9350-6>

490 Fernández-Sevilla, J.M., Brindley, C., Jiménez-Ruíz, N., Acien, F.G., 2018. A simple
491 equation to quantify the effect of frequency of light/dark cycles on the photosynthetic
492 response of microalgae under intermittent light. *Algal Res.* 35, 479–487.
493 <https://doi.org/10.1016/j.algal.2018.09.026>

494 Foladori, P., Petrini, S., Andreottola, G., 2018. Evolution of real municipal wastewater
495 treatment in photobioreactors and microalgae-bacteria consortia using real-time
496 parameters. *Chem. Eng. J.* 345, 507–516. <https://doi.org/10.1016/j.cej.2018.03.178>

497 Galès, A., Bonnafous, A., Carré, C., Jauzein, V., Lanouguère, E., Le, E., Pinoit, J., Poullain,
498 C., Roques, C., Sialve, B., Simier, M., Steyer, J., Fouilland, E., 2019. Importance of
499 ecological interactions during wastewater treatment using High Rate Algal Ponds under
500 different temperate climates. *Algal Res.* 40, 101508.
501 <https://doi.org/10.1016/j.algal.2019.101508>

502 González-Camejo, J., Jiménez-Benítez, A., Ruano, M. V., Robles, A., Barat, R., Ferrer, J.,
503 2019. Optimising an outdoor membrane photobioreactor for tertiary sewage treatment. *J.*
504 *Environ. Manage.* 245, 76–85. <https://doi.org/10.1016/j.jenvman.2019.05.010>

505 Honda, R., Boonnorat, J., Chiemchaisri, C., Chiemchaisri, W., Yamamoto, K., 2012. Carbon
506 dioxide capture and nutrients removal utilizing treated sewage by concentrated
507 microalgae cultivation in a membrane photobioreactor. *Bioresour. Technol.* 125, 59–64.
508 <https://doi.org/10.1016/j.biortech.2012.08.138>

509 Kumar, K., Mishra, S.K., Shrivastav, A., Park, M.S., Yang, J.W., 2015. Recent trends in the
510 mass cultivation of algae in raceway ponds. *Renew. Sustain. Energy Rev.* 51, 875–885.
511 <https://doi.org/10.1016/j.rser.2015.06.033>

512 Lazarova, V., Choo, K.-H., Cornel, P., 2012. Water-Energy Interactions in Water Reuse.
513 <https://doi.org/10.2166/9781780400662>

514 Liao, Y., Bokhary, A., Maleki, E., Liao, B., 2018. A review of membrane fouling and its

515 control in algal-related membrane processes. *Bioresour. Technol.* 264, 343–358.
516 <https://doi.org/10.1016/j.biortech.2018.06.102>

517 Luo, Y., Le-Clech, P., Henderson, R.K., 2017. Simultaneous microalgae cultivation and
518 wastewater treatment in submerged membrane photobioreactors: A review. *Algal Res.*
519 24, 425–437. <https://doi.org/10.1016/J.ALGAL.2016.10.026>

520 Marbelia, L., Bilad, M.R., Passaris, I., Discart, V., Vandamme, D., Beuckels, A., Muylaert,
521 K., Vankelecom, I.F.J., 2014. Membrane photobioreactors for integrated microalgae
522 cultivation and nutrient remediation of membrane bioreactors effluent. *Bioresour.*
523 *Technol.* 163, 228–235. <https://doi.org/10.1016/j.biortech.2014.04.012>

524 Mata, T.M., Martins, A.A., Caetano, N.S., 2010. Microalgae for biodiesel production and
525 other applications: A review. *Renew. Sustain. Energy Rev.* 14, 217–232.
526 <https://doi.org/10.1016/J.RSER.2009.07.020>

527 Nopens, I., Capalozza, C., Vanrolleghem, P.A., 2001. Stability analysis of a synthetic
528 municipal wastewater. *Gent.* <https://doi.org/10.1017/CBO9781107415324.004>

529 Novoveská, L., Zapata, A.K.M., Zabolotney, J.B., Atwood, M.C., Sundstrom, E.R., 2016.
530 Optimizing microalgae cultivation and wastewater treatment in large-scale offshore
531 photobioreactors. *Algal Res.* 18, 86–94. <https://doi.org/10.1016/j.algal.2016.05.033>

532 Perin, G., Cimetta, E., Monetti, F., Morosinotto, T., Bezzo, F., 2016. Novel micro-
533 photobioreactor design and monitoring method for assessing microalgae response to light
534 intensity. *Algal Res.* 19, 69–76. <https://doi.org/10.1016/j.algal.2016.07.015>

535 Pretel, R., Robles, A., Ruano, M. V., Seco, A., Ferrer, J., 2016. A plant-wide energy model for
536 wastewater treatment plants: application to anaerobic membrane bioreactor technology.
537 *Environ. Technol.* 37, 2298–2315. <https://doi.org/10.1080/09593330.2016.1148903>

538 Ras, M., Steyer, J.P., Bernard, O., 2013. Temperature effect on microalgae: A crucial factor
539 for outdoor production. *Rev. Environ. Sci. Biotechnol.* 12, 153–164.
540 <https://doi.org/10.1007/s11157-013-9310-6>

541 Robles, A., Capson-Tojo, G., Ruano, M. V., Seco, A., Ferrer, J., 2018. Real-time optimization
542 of the key filtration parameters in an AnMBR: urban wastewater mono-digestion vs. co-
543 digestion with domestic food waste. *Waste Manag.* 80, 299–309.
544 <https://doi.org/10.1016/j.wasman.2018.09.031>

545 Robles, A., Ruano, M. V., Ribes, J., Seco, A., Ferrer, J., 2014. Model-based automatic tuning
546 of a filtration control system for submerged anaerobic membrane bioreactors (AnMBR).
547 *J. Memb. Sci.* 465, 14–26. <https://doi.org/10.1016/j.memsci.2014.04.012>

548 Salama, E.S., Kurade, M.B., Abou-Shanab, R.A.I., El-Dalatony, M.M., Yang, I.S., Min, B.,
549 Jeon, B.H., 2017. Recent progress in microalgal biomass production coupled with
550 wastewater treatment for biofuel generation. *Renew. Sustain. Energy Rev.* 79, 1189–
551 1211. <https://doi.org/10.1016/j.rser.2017.05.091>

552 Seco, A., Aparicio, S., González-Camejo, J., Jiménez-Benítez, A., Mateo, O., Mora, J.F.,
553 Noriega-Hevia, G., Sanchis-Perucho, P., Serna-García, R., Zamorano-López, N.,
554 Giménez, J.B., Ruiz-Martínez, A., Aguado, D., Barat, R., Borrás, L., Bouzas, A., Martí,
555 N., Pachés, M., Ribes, J., Robles, A., Ruano, M. V., Serralta, J., Ferrer, J., 2018.
556 Resource recovery from sulphate-rich sewage through an innovative anaerobic-based
557 water resource recovery facility (WRRF). *Water Sci. Technol.* 78, 1925–1936.
558 <https://doi.org/10.2166/wst.2018.492>

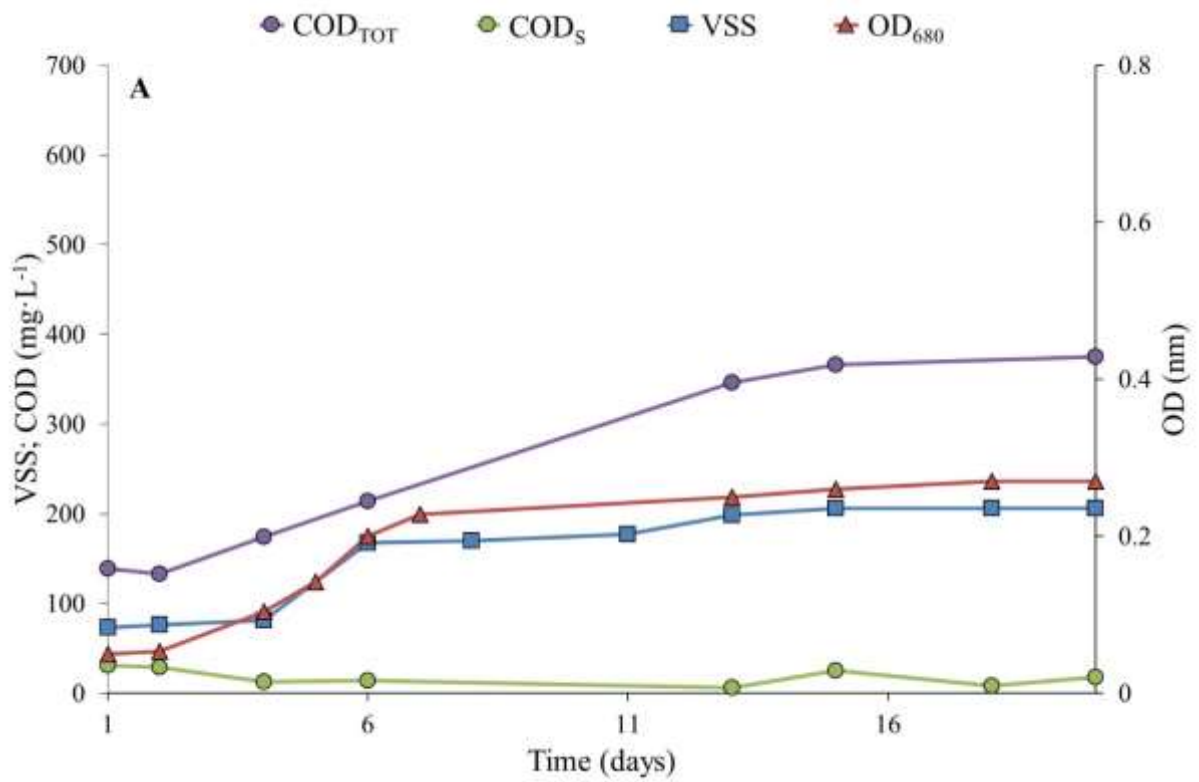
- 559 Sheng, A.L.K., Bilad, M.R., Osman, N.B., Arahman, N., 2017. Sequencing batch membrane
560 photobioreactor for real secondary effluent polishing using native microalgae: Process
561 performance and full-scale projection. *J. Clean. Prod.* 168, 708–715.
562 <https://doi.org/10.1016/j.jclepro.2017.09.083>
- 563 Shoener, B.D., Schramm, S.M., Béline, F., Bernard, O., Martínez, C., Plósz, B.G., Snowling,
564 S., Steyer, J.P., Valverde-Pérez, B., Wágner, D., Guest, J.S., 2019. Microalgae and
565 cyanobacteria modeling in water resource recovery facilities: A critical review. *Water*
566 *Res. X* 2. <https://doi.org/10.1016/j.wroa.2018.100024>
- 567 Solimeno, A., García, J., 2017. Microalgae-bacteria models evolution: From microalgae
568 steady-state to integrated microalgae-bacteria wastewater treatment models – A
569 comparative review. *Sci. Total Environ.* <https://doi.org/10.1016/j.scitotenv.2017.07.114>
- 570 Sun, L., Tian, Y., Zhang, J., Cui, H., Zuo, W., Li, J., 2018. A novel symbiotic system
571 combining algae and sludge membrane bioreactor technology for wastewater treatment
572 and membrane fouling mitigation: Performance and mechanism. *Chem. Eng. J.* 344,
573 246–253. <https://doi.org/10.1016/j.cej.2018.03.090>
- 574 Sun, X., Wang, C., Tong, Y., Wang, W., Wei, J., 2013. A comparative study of microfiltration
575 and ultrafiltration for algae harvesting. *Algal Res.* 2, 437–444.
576 <https://doi.org/10.1016/j.algal.2013.08.004>
- 577 Turon, V., Trably, E., Fayet, A., Fouillard, E., Steyer, J.P., 2015. Raw dark fermentation
578 effluent to support heterotrophic microalgae growth: Microalgae successfully
579 outcompete bacteria for acetate. *Algal Res.* 12, 119–125.
580 <https://doi.org/10.1016/j.algal.2015.08.011>
- 581 Viruela, A., Robles, Á., Durán, F., Ruano, M.V., Barat, R., Ferrer, J., Seco, A., 2018.
582 Performance of an outdoor membrane photobioreactor for resource recovery from
583 anaerobically treated sewage. *J. Clean. Prod.* 178, 665–674.
584 <https://doi.org/10.1016/j.jclepro.2017.12.223>
- 585 Wang, Y., Guo, W., Yen, H.W., Ho, S.H., Lo, Y.C., Cheng, C.L., Ren, N., Chang, J.S., 2015.
586 Cultivation of *Chlorella vulgaris* JSC-6 with swine wastewater for simultaneous
587 nutrient/COD removal and carbohydrate production. *Bioresour. Technol.* 198, 619–625.
588 <https://doi.org/10.1016/j.biortech.2015.09.067>
- 589 Wang, Y., Ho, S.-H., Cheng, C.-L., Guo, W.-Q., Nagarajan, D., Ren, N.-Q., Lee, D.-J.,
590 Chang, J.-S., 2016. Perspectives on the feasibility of using microalgae for industrial
591 wastewater treatment. *Bioresour. Technol.* 222, 485–497.
592 <https://doi.org/10.1016/J.BIORTECH.2016.09.106>
- 593 Wicaksana, F., Fane, A.G., Pongpairroj, P., Field, R., 2012. Microfiltration of algae (*Chlorella*
594 *sorokiniana*): Critical flux, fouling and transmission. *J. Memb. Sci.* 387–388, 83–92.
595 <https://doi.org/10.1016/j.memsci.2011.10.013>
- 596 Yang, J., Gou, Y., Fang, F., Guo, J., Lu, L., Zhou, Y., Ma, H., 2018. Potential of wastewater
597 treatment using a concentrated and suspended algal-bacterial consortium in a photo
598 membrane bioreactor. *Chem. Eng. J.* 335, 154–160.
599 <https://doi.org/10.1016/j.cej.2017.10.149>

600

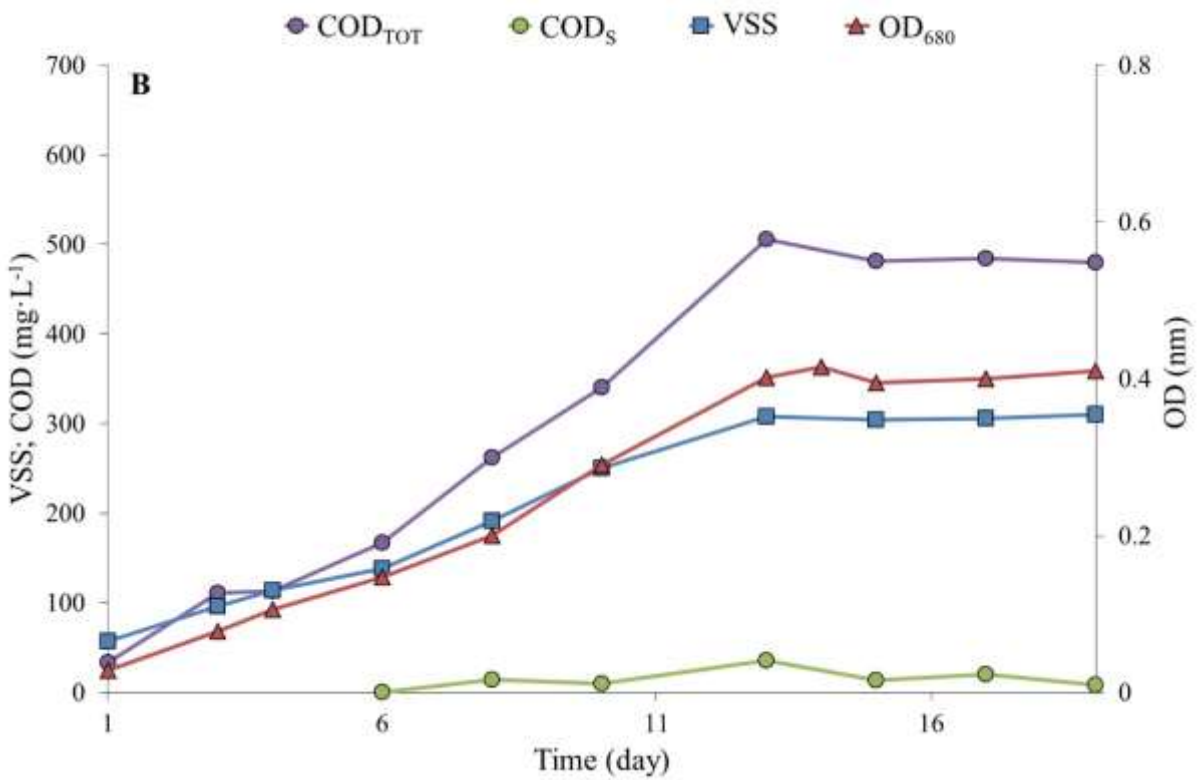
601

602 Figure and table captions

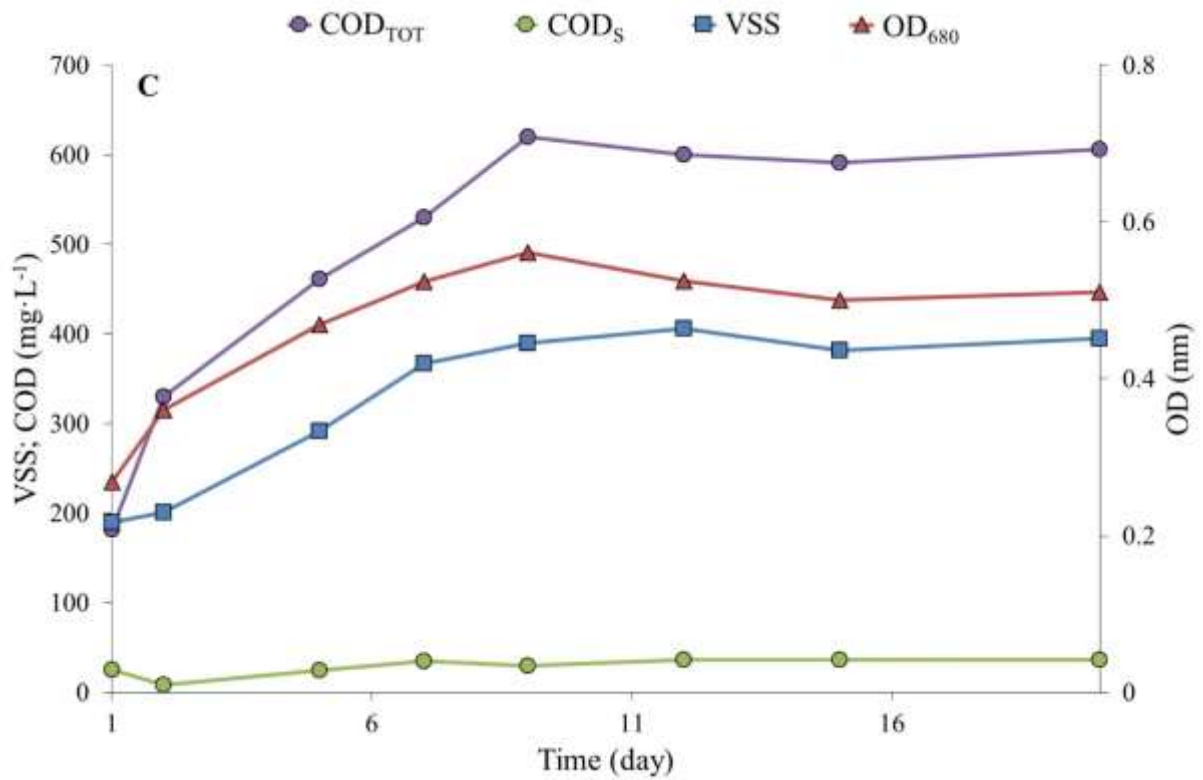
603



604



605

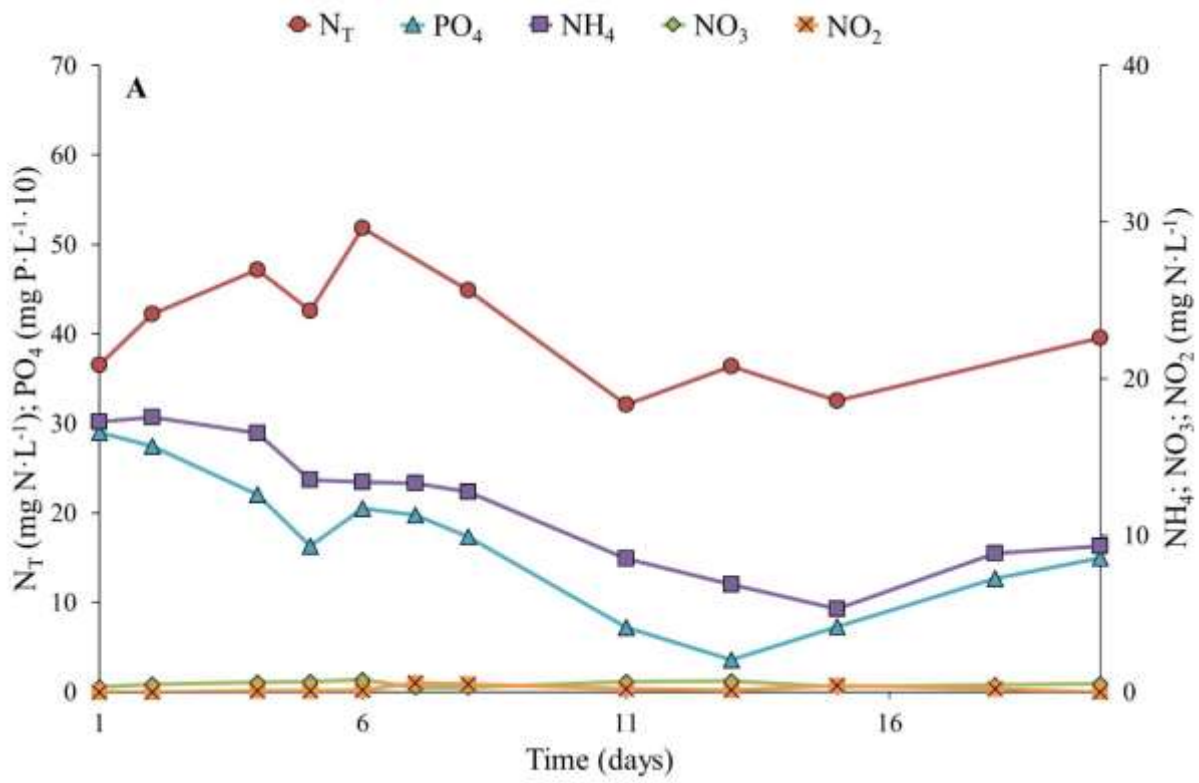


606

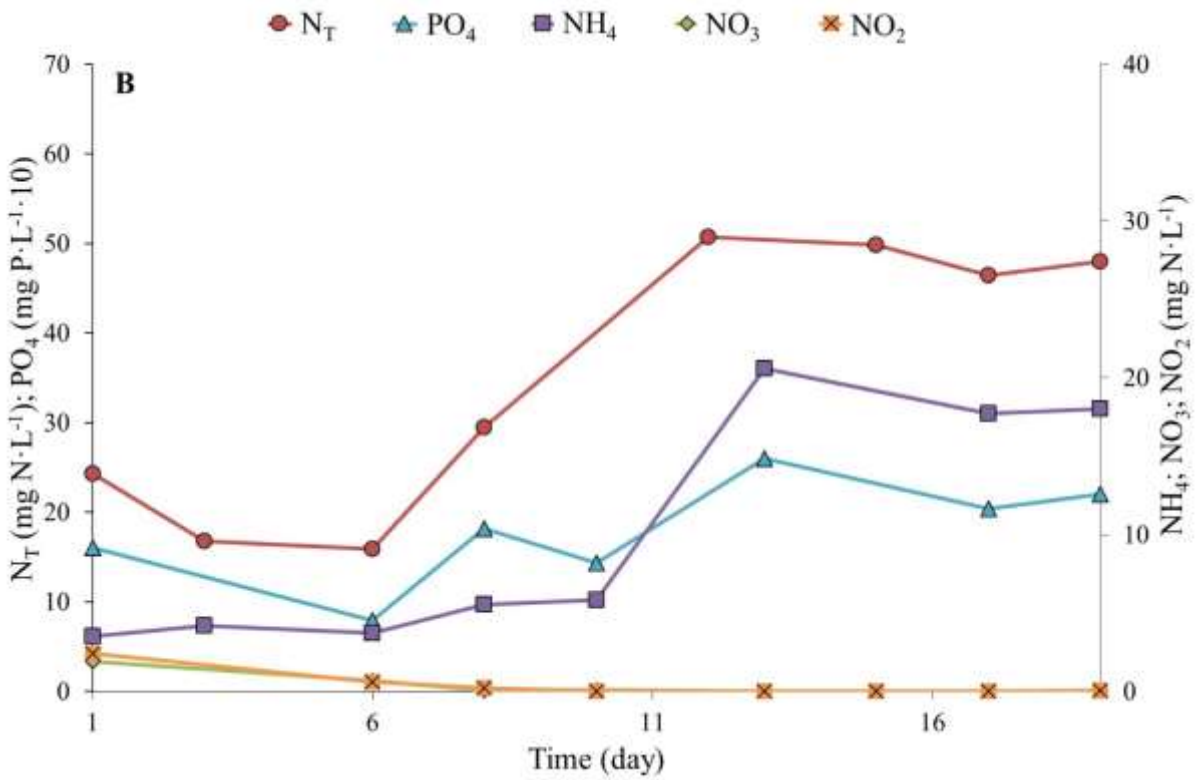
607 **Figure 1.** M-HRAP performance when operating at a BRT of 6 days and HRTs of (A) 6, (B)
 608 4, and (C) 2.5 days. COD_{TOT}: total chemical oxygen demand; COD_S: soluble chemical oxygen
 609 demand; VSS: volatile suspended solids; OD₆₈₀: optical density at 680 nm

610

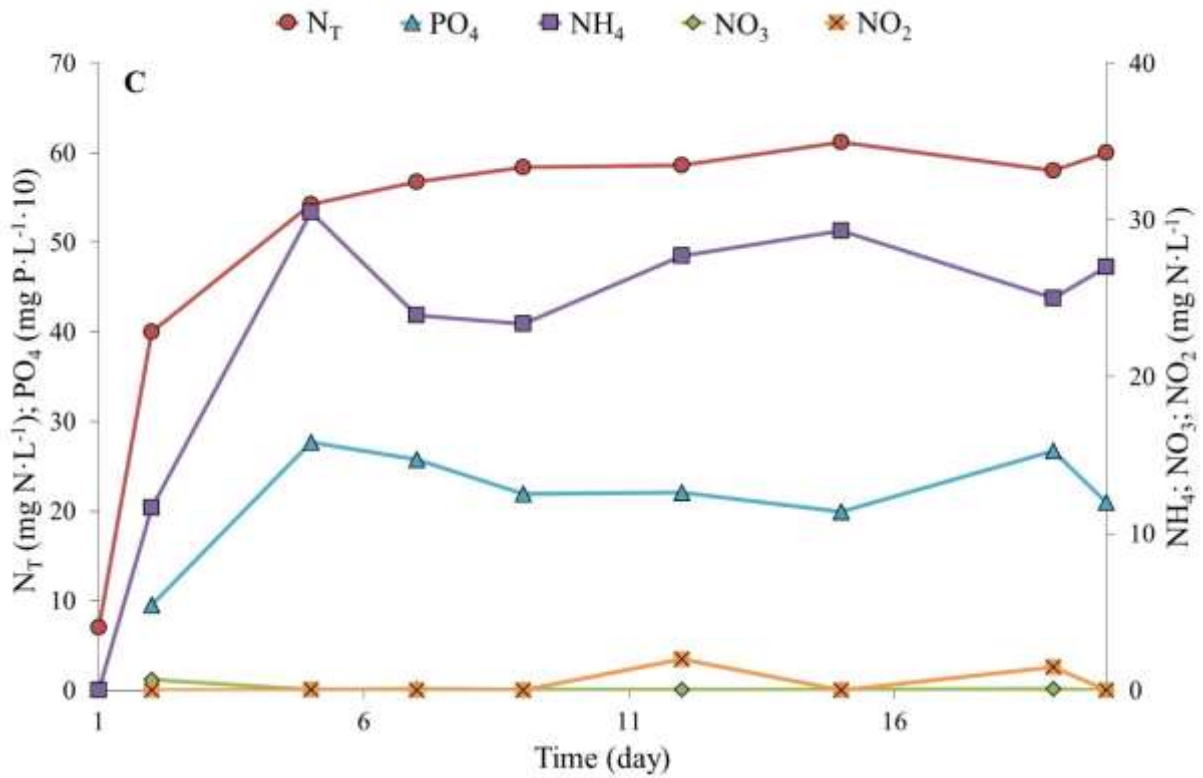
611



612

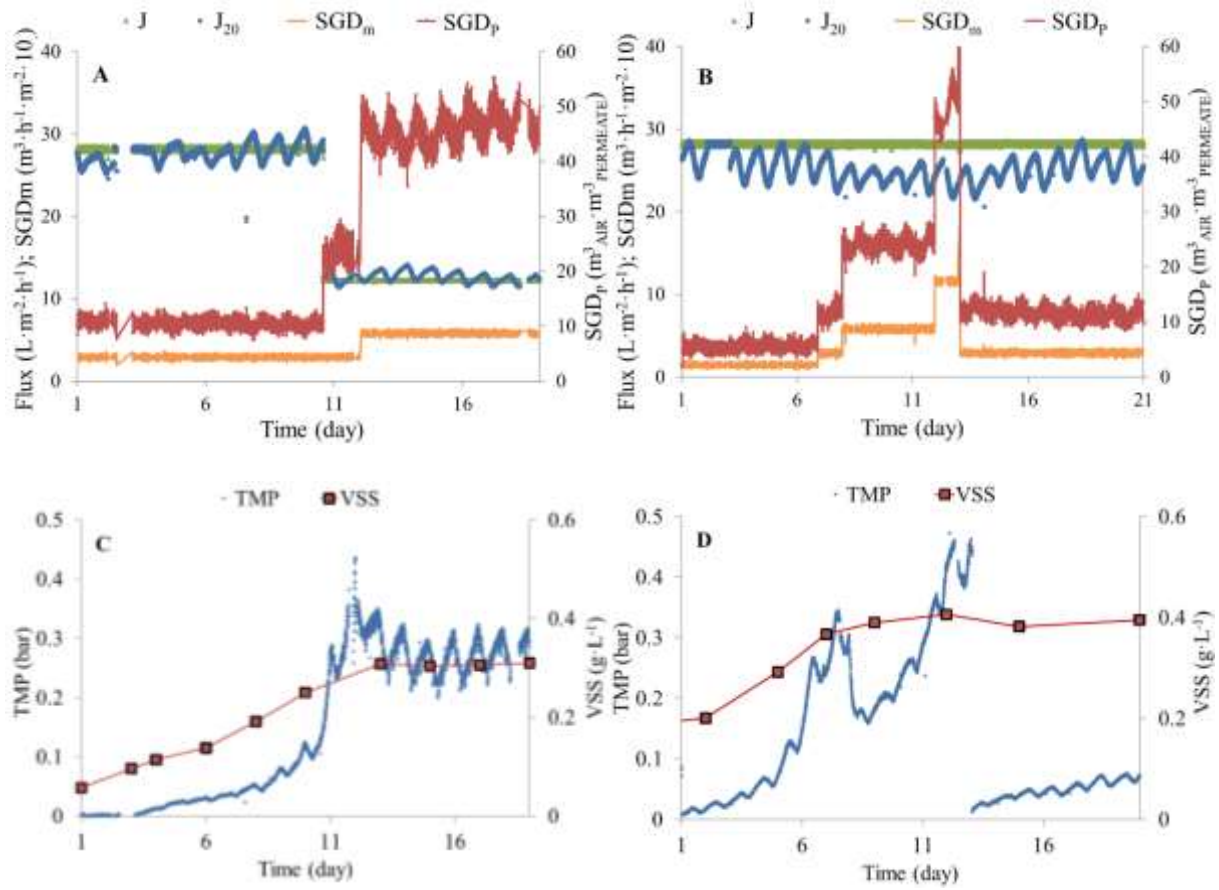


613



614
 615
 616
 617
 618
 619

Figure 2. M-HRAP performance when operating at a BRT of 6 days and HRTs of (A) 6, (B) 4, and (C) 2.5 days. The evolutions of the concentrations of total nitrogen (N_T) in the mixed liquor and the inorganic nutrients (NH_4 -N, PO_4 -P, NO_3 -N and NO_2 -N) in the effluent are given



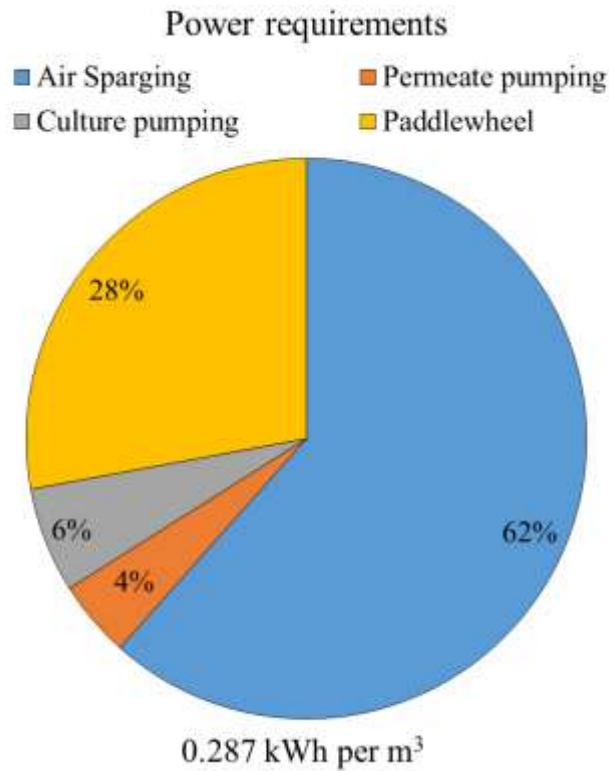
620

621

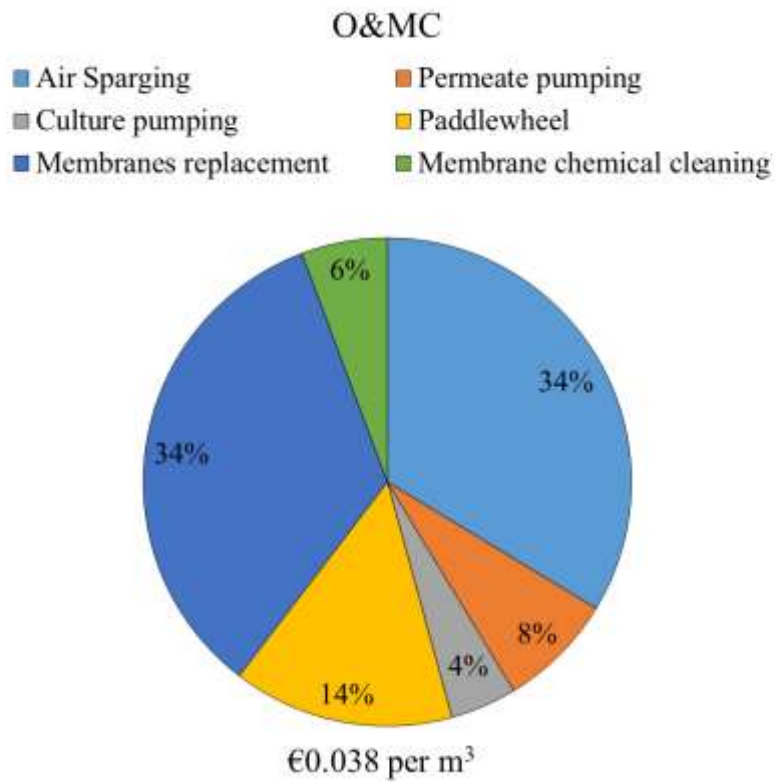
622 **Figure 3.** Evolution of J , J_{20} , SAD_m and SAD_p during (A) run II and (B) run III. The TMP
 623 and the VSS concentration (C) run II and (D) run III are also presented

624

625



626



627 **Figure 4.** (A) Power requirements and (B) operational and maintenance costs (O&MC) for a
628 full-scale plant design with a treatment capacity of 1,000 m³·d⁻¹. $J_{20} = 28 \text{ L} \cdot \text{m}^{-3} \cdot \text{h}^{-1}$; $\text{SAD}_m =$
629 $0.25 \text{ m}^3 \cdot \text{m}^{-2} \cdot \text{h}^{-1}$

630

631 **Table 1.** Average operating conditions and objectives of the different run periods

Run	Objective	BRT (d)	HRT (d)	J (L·m ⁻² ·h ⁻¹)	SAD _m (m ³ ·m ⁻² ·h ⁻¹)	Solar irradiance (μE·m ⁻² ·s ⁻¹)	Temperature (°C)
I		6	6	NA	NA	433±113	22.0±3.1
II	Evaluate effect of BRT and HRT decoupling	6	4	28, 14	0.3, 0.6	395±72	21.2±2.0
III		6	2.5	28	0.12 – 1.0	420±90	24.5±1.8
IV	Evaluate effect of light and temperature changes	6	2.5	27-31	0.6 – 1.2	253±195	14.1±1.1

632 BRT stands for biological retention time, HRT for hydraulic retention time, J for trans membrane flux, SAD_m for
 633 the specific air demand per membrane unit and NA not applicable

634

635

636 **Table 2.** Average results in runs I to IV at pseudo-steady state for: nitrogen and phosphorous
 637 removal rates, biomass productivities, photosynthetic efficiency, and carbon dioxide
 638 biofixation

Run	HRT (d)	T (°C)	Solar irradiance ($\mu\text{E}\cdot\text{m}^{-2}\cdot\text{s}^{-1}$)	NRR ($\text{g N}\cdot\text{m}^{-3}\cdot\text{d}^{-1}$)	PRR ($\text{g P}\cdot\text{m}^{-3}\cdot\text{d}^{-1}$)	Biomass productivity ($\text{g VSS}\cdot\text{m}^{-3}\cdot\text{d}^{-1}$)	PE (%)	CO _{2BF} ($\text{kg CO}_2\cdot\text{m}^{-3}$)
I	6	22.0±3.1	433±113	3.9±0.7	0.54±0.05	30.1±0.4	1.0±0.1	0.20±0.00
II	4	21.2±2.0	395±72	7.8±1.3	1.30±0.20	66.2±1.8	4.1±0.2	0.31±0.01
III	2.5	24.5±1.8	420±90	11.0±1.3	1.55±0.09	95.1±1.7	3.5±0.2	0.39±0.01
IV	2.5	14.1±1.1	253±195	8.0±1.2	1.1±0.12	65.3±1.7	3.9±0.2	0.29±0.01

639 HRT stands for hydraulic retention time, T for temperature, NRR for nitrogen removal rate, PRR for
 640 phosphorous removal rate, PE for photosynthetic efficiency, CO_{2BF} for carbon dioxide biofixation, and VSS for
 641 volatile suspended solids
 642